Realizing Fresnel Incoherent Correlation Holography as a Coded Aperture Imaging System Using Advanced Computational Algorithms

Francis Gracy Arockiaraj
Institute of Physics, University of Tartu,
Estonia.
School of Electrical and Computer Engineering, Ben Gurion University of the Negev,
Israel.
francis.gracy.arockiaraj@ut.ee

Agnes Pristy Ignatius Xavier
Institute of Physics, University of Tartu,
Estonia.
School of Electrical and Computer Engineering, Ben Gurion University of the Negev,
Israel.
agnes.pristy.ignatius.xavier@ut.ee

Shivasubramanian Gopinath
Institute of Physics, University of Tartu,
Estonia.
shivasubramanian.gopinath@ut.ee

Aravind Simon John Francis Rajeswary
Institute of Physics, University of Tartu,
Estonia.
aravind@ut.ee

Saulius Juodkazis
Optical Sciences Center and ARC Training Centre in Surface Engineering for Advanced Materials (SEAM), Swinburne University of Technology,
Australia.
Tokyo Tech World Research Hub Initiative (WRHI), School of Materials and Chemical Technology, Tokyo Institute of Technology,
Japan
sjuodkazis@swin.edu.au

Vijayakumar Anand
Institute of Physics, University of Tartu,
Estonia.
Optical Sciences Center and ARC Training Centre in Surface Engineering for Advanced Materials (SEAM), Swinburne University of Technology,
Australia.
vijayakumar.anand@ut.ee

***Abstract*— Fresnel incoherent correlation holography (FINCH) also called as incoherent digital holography. In FINCH, a self-interference Fresnel hologram is created when light from an object point is split into two, modulated using two different quadratic phase masks and interfered. At least three such holograms are needed with phase shifts 0, $2\pi/3$ and $4\pi/3$ and combined to remove the twin image and bias terms during computational reconstruction involving Fresnel backpropagation. When the FINCH setup is engineered to achieve the same beam diameter for the two interfering beams, a super lateral resolution which is 1.5 times that of a direct imaging system for the same numerical aperture, is obtained. FINCH has a low temporal and axial resolution and low light throughput when compared to the direct imaging system. In this study, FINCH is enhanced and realized as a coded aperture imaging (CAI) system using three computational algorithms: Transport of Amplitude into Phase based on Gerchberg Saxton Algorithm (TAP-GSA), Lucy-Richardson-Rosen algorithm (LRRA) and computational point spread function engineering (CPSFE) technique. The PSF is recorded for FINCH in the first step as in CAI and used as the reconstruction function. The TAP-GSA was used to improve the design of phase masks and achieve a high light throughput. The CPSFE was used to shift the lateral resolution limit from the diameter of the pinhole which is used for recording the PSF to the limit of FINCH. The LRRA was used for the reconstruction of FINCH holograms. Optical experimental results of CAI-inspired 'perfect' FINCH are promising for applications in fluorescence microscopy.**

Keywords—Coded aperture imaging (CAI), diffractive optics, FINCH with CAI, PSF engineering.

I. INTRODUCTION

Fresnel incoherent correlation holography (FINCH) also called as incoherent digital holography was developed in 2007 by Joseph Rosen of Ben Gurion University and Gary Brooker of John Hopkins University [1]. In FINCH, a spatially incoherent light source is used to illuminate the object. Here, the light from the object point is modulated by two different quadratic phase masks, creating two object waves that are obtained from the same object point. These object waves interfere to form a self-interference hologram. The interference pattern contains 3D location information of the object point. For multiple points, there are multiple self-interference patterns that are summed in the image sensor. In the first version of FINCH [1], a random multiplexing approach was used to combine two quadratic phase masks with different focal distances with different phase shifts, namely 0, $2\pi/3$, and $4\pi/3$. The phase masks were displayed on a spatial light modulator (SLM) one after the other, and the corresponding phase-shifted holograms were recorded. These holograms were superposed to form a complex hologram. Eventually, the object information is retrieved without twin image and bias terms by numerically backpropagating the complex hologram to one of the two focal planes. However, this random multiplexing approach had a low signal-to-noise ratio (SNR). The SNR of FINCH was later improved using the polarization multiplexing method [2], wherein two polarizers were oriented at 45° with respect to the active axis of the SLM, and these polarizers were placed one before and one after the SLM. The first polarizer allows the light that is oriented 45°

This research has received funding from the European Union's Horizon 2020 research and innovation programme under grant agreement No 857627 (CIPHR)

2023 International Conference on Next Generation Electronics (NEleX) | 979-8-3503-1908-8/23/$31.00 ©2023 IEEE | DOI: 10.1109/NELEX59773.2023.10421576

wherein, nearly 50% of the light gets modulated, and the remaining propagates without any modulation. Interference occurs between this modulated and unmodulated light at the second polarizer. Though this method possesses a high SNR, it comes with a trade-off of less light throughput due to the two polarizers. During polarization multiplexing in FINCH, it was also discovered that FINCH has super-resolution when the two beams' diameters are perfectly matched at the image sensor. The lateral resolution of FINCH was reported to be twice that of coherent imaging systems and 1.5 times that of incoherent imaging systems with same numerical aperture (NA). However, the axial resolution of FINCH is lower than that of direct incoherent imaging systems. FINCH has evolved over the past years with improved temporal resolution owing to the contributions of various researchers [3]. A 4-pol image sensor was used to capture all four phase-shifted holograms 0, $\pi/4$, $\pi/2$ and $3\pi/4$ simultaneously in a single camera shot followed by an interpolation approach to obtain the missing pixel information [3]. This approach demonstrated a temporal resolution three times that of [1] but suffered from a low SNR. Then, a checkerboard grating was utilized to spatially multiplex numerous camera shots to a single shot with a trade-off of a low field of view [3]. Then, FINCH was implemented with a birefringent crystal lens [3], wherein α-barium borate and calcite crystals were utilized to replace the SLM. The results produced from these liquid crystal elements were better, but the material availability makes it difficult to implement. In all the above studies, the temporal resolution of FINCH was enhanced either by sacrificing SNR or field of view.

A two-step phase-shifting technique was developed to enhance the temporal resolution of FINCH by 1.5 times compared to [1] without sacrificing the SNR or field of view [3]. Later, single-shot FINCH was reported by realizing FINCH as a coded aperture imaging (CAI) system for the first time using non-linear reconstruction (NLR) [3]. As required by CAI systems, the point spread hologram (PSH) library was recorded for all axial locations in the first step. In the second step, a single object hologram was recorded. The object is reconstructed by applying NLR on the recorded PSH library and the single object hologram. This approach was derived from coded aperture correlation holography (COACH) [2]. In this approach [3], random multiplexing was used, and the device was manufactured using electron beam lithography. Consequently, the SNR was lower than the polarization multiplexing method and had a low light throughput.

Consolidating the above developments, the current state-of-the-art FINCH consists of higher lateral resolution and lower axial resolution compared to an incoherent direct imaging system. FINCH has half of the temporal resolution and one-fourth of the light throughput of that of incoherent direct imaging systems [2, 3]. It should be noted that it is possible to enhance the temporal resolution by the above techniques by sacrificing either the SNR or field of view. The above limitations in FINCH preclude its implementation in many application areas.

In this study, FINCH has been realized as CAI again similar to [3] but implemented with three advanced computational methods: Transport of Amplitude into Phase based on Gerchberg Saxton Algorithm (TAP-GSA) for designing phase masks [4], Lucy-Richardson-Rosen algorithm (LRRA) for image reconstruction from FINCH holograms [5] and computational point spread function engineering (CPSFE) technique for engineering PSH, to reach the resolution limit beyond the diameter of the pinhole used to record the PSH. The simultaneous application of the above methods enhances FINCH along all the facets while retaining its super lateral resolution. The implementation of FINCH as CAI improves the axial resolution and temporal resolution to those of direct incoherent imaging. The TAP-GSA enables multiplexing two quadratic phase masks with a high light throughput. The LRRA enables hologram reconstruction with a high SNR. The CPSFE solves a fundamental problem in CAI, allowing to reach the resolution of FINCH beyond the diameter of the pinhole used for recording the PSH. The methodology is presented in the next section. Experimental results for single-plane, three-dimensional imaging, and PSF engineering are presented in the third section. The conclusion and future perspectives are presented in the final section.

II. Methodology

The optical configuration of FINCH is displayed in Fig. 1. The light from a spatially incoherent light source reaches lens L1, which critically illuminates the object. The light from the object point is collimated by lens L2 and reaches the SLM after being polarized concerning the active axis of SLM by a polarizer P_1. On the SLM, the phase mask is displayed, which is created using the TAP-GSA algorithm by combining two quadratic phase masks. The schematic of the TAP-GSA algorithm is shown in Fig. 2. Through TAP-GSA, the two quadratic phase masks are summed, and the resulting complex function is converted into a phase-only function by iteratively transferring the amplitude information into the phase. In the first step, the ideal complex function is calculated by performing an algebraic sum of phase-only quadratic phase functions, and the intensity and phase distributions are calculated at a plane of interest using the Fresnel transform [2]. After this calculation, the intensity constraints are applied in both planes – uniform intensity in the mask plane and intensity calculated for ideal complex function in the sensor plane. A partial phase constraint is applied in the sensor domain. The algorithm is iterated until a pure phase function is obtained in the mask domain. Two object waves are generated at the SLM, and interference occurs between these two waves at the image sensor. The PSH and the object hologram (OH) are recorded. The PSH and OH are processed by the LRRA. The schematic of LRRA is shown in Fig. 3. The LRRA is formed from Lucy-Richardson algorithm (LRA) and NLR.

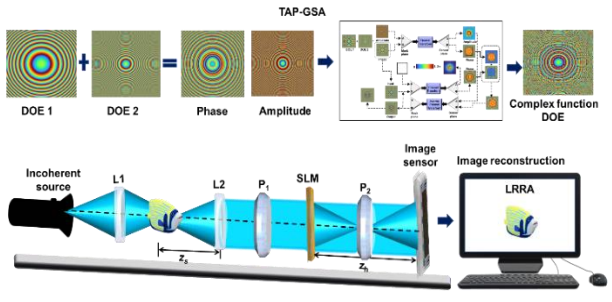

Fig. 1. Optical set-up of FINCH with TAP-GSA and LRRA. L1, L2 - refractive lenses; P_1, P_2 – polarizer.

The LRA consists of a forward convolution and a backward correlation. The forward convolution is initiated with an initial guessed solution which is the OH. The OH is convolved with the PSH and the ratio of it with OH is obtained. This result is correlated with the PSH, and the outcome is multiplied to the

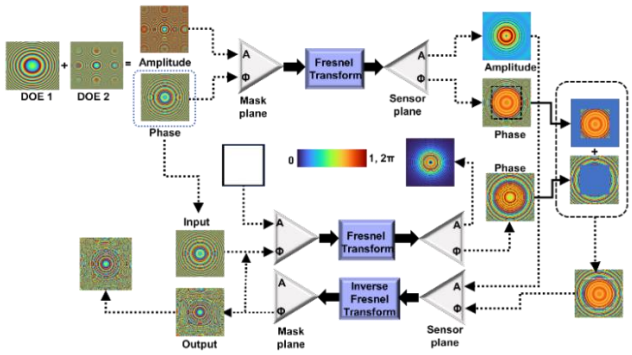

Fig. 2. Schematic of Transport of Amplitude into Phase based on Gerchberg Saxton Algorithm (TAP-GSA) algorithm. A represents magnitude and Φ represents phase. DOE1 and DOE2 are the two quadratic phase masks.

previous solution which is the OH. This procedure continues until the solution attains convergence to an optimal solution. In LRRA, the correlation is replaced by NLR whose parameters can be controlled by α and β. LRA requires only one parameter optimization, which is the number of iterations n. NLR requires two parameter optimizations: α and β. In LRRA, there are three parameter optimizations: α and β and n.

Considering again that LRA consists of a forward convolution and a backward correlation. During backward correlation, most of the information is present in the phase of the spectrum, and the magnitude of the spectrum contributes to the SNR. In a regular correlation, there is no option to tune the magnitude of the spectrum, resulting in a solution that is not optimal. In LRRA, the backward correlation is replaced by NLR, in which the magnitudes of the spectrum of the two matrices can be tuned. This improvement in the backward operation impacts the algorithm resulting in a better estimation, rapid convergence, and improved SNR. LRA and NLR are based on two different approaches. In LRA, the relation between OH, O, and PSH is gradually improved, starting from an initially guessed object O to the optimal result iteratively until the estimated O satisfies the convolution relation between the three matrices. In NLR, the optimal solution is obtained using a figure of merit 'entropy,' which only finds the case with maximum SNR but does not validate the relational information between the three matrices. This difference in approach results in different performances of LRA and NLR. In LRRA, the SNR of backward correlation is improved by replacing it with NLR resulting in better performance than LRA and NLR. However, further studies are needed for a better understanding of the differences in performances.

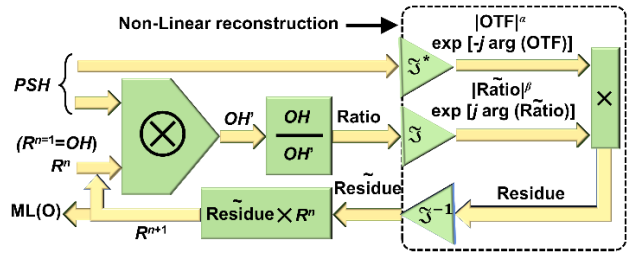

Fig. 3. Schematic of Lucy-Richardson-Rosen algorithm.

III. Results

The experimental components are similar to [6]. The light from the high-power LED passed through a refractive lens and critically illuminated the object. Element '1' in group 5 of the United States Air Force (USAF) target was used as the test object. The light from the object is passed through the polarizer, which allows light only along the active axis of the SLM and reaches the beam splitter. The beam splitter splits the incoming beam into two beams, wherein one of the two beams reaches the SLM. In the SLM, the phase mask generated from the TAP-GSA was displayed. The PSHs were recorded in the first step at two axial locations, and the OHs were recorded in the next step using the two USAF objects at the two locations where PSHs were recorded.

A. Experimental Results for Single-Plane Imaging

The experimental result for single plane imaging with z_s = 5 cm is shown in Fig. 4. It was carried out for the USAF test object '1' of group 5. The phase masks were synthesized for degrees of freedom (DOF) 98% using TAP-GSA which is shown in Fig. 4a. DOF is characterized as the proportion of pixels substituted within the phase matrix on the image sensor to the overall pixel count within that matrix. The PSH, OH for z_s = 5 cm are shown in Figs. 4b and 4c respectively. The reconstruction result for object "1" achieved from LRRA for $\alpha = 0.2, \beta = 0.9, n = 9$, and direct imaging result are shown in Figs. 4d and 4e respectively.

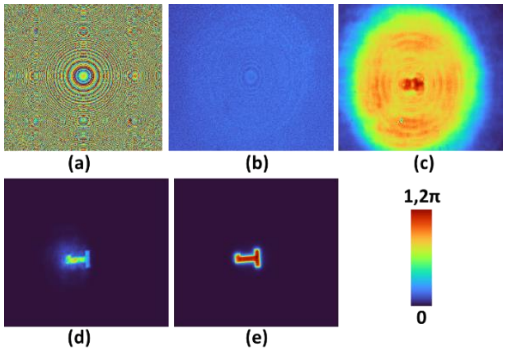

Fig. 4. Experimental results for single plane imaging. (a) phase mask with a DOF of 98% generated from TAP-GSA algorithm. (b) PSH recorded for z_s = 5 cm. (c) OH for the object at z_s = 5 cm. (d) Reconstruction result using PSH recorded for z_s = 5 cm. (e) Direct image (DI).

B. 3-Dimensional Imaging

The 3-dimensional imaging was carried out using objects "3" and "1" at two different distances, z_s = 5 cm and z_s = 5.6 cm. The PSHs corresponding to the above distances are shown in Figs. 5a. and 5b. The OH is shown in Fig. 5c. The reconstruction results for distances z_s = 5 cm and z_s = 5.6 cm are shown in Figs. 5d and 5e respectively. Figure 5f. shows the direct imaging result when the two objects are in the same plane. The optimal reconstruction results were obtained from LRRA for $\alpha = 0.2, \beta = 1$, and $n = 11$. The magnitude and phase of the conventional FINCH complex hologram are shown in Figs. 5g and 5h respectively. The reconstruction result of conventional FINCH by Fresnel backpropagation is shown in Fig. 5i. Comparing the reconstruction results obtained for conventional FINCH with FINCH as CAI shows an improvement in axial resolution.

C. Experimental Results for Computational Point Spread Function Engineering (CPSFE)

The ideal PSH is engineered from the recorded PSH using a pinhole with a diameter d = 50 µm by treating the PSH itself as OH and applying LRRA to estimate the ideal PSH. There are two known matrices, namely recorded PSH and DI of the pinhole. Using LRRA, the ideal PSH was estimated. The recorded PSH is shown in Fig. 6a.

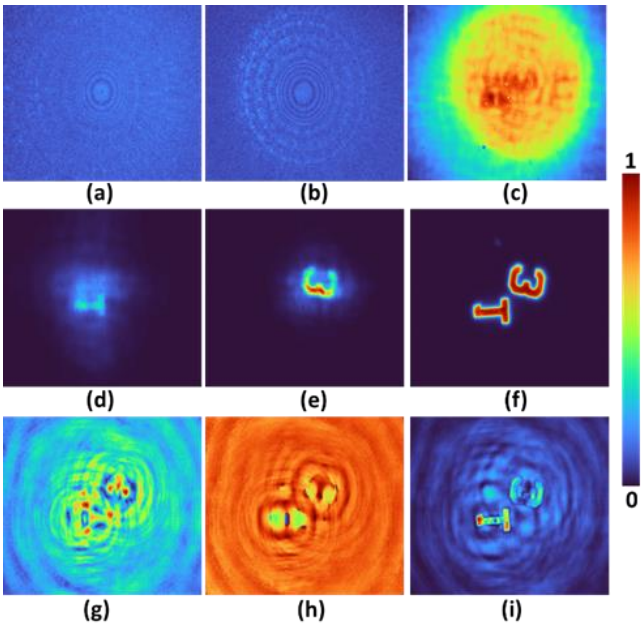

Fig. 5. 3-D reconstruction results. PSH recorded for (a) z_s = 5 cm and (b) z_s = 5.6 cm. (c) OH for the object with two planes. (d) Reconstruction result using PSH recorded for z_s = 5 cm. (e) Reconstruction result using PSH recorded for z_s = 5.6 cm. (f) DI when the objects lies in identical plane. (g) Magnitude and (h) phase of complex hologram. (i) Reconstruction result for conventional FINCH.

The engineered ideal PSH shown in Fig. 6b is obtained from LRRA for α = 0.4, β = 1, n = 10. The recorded OH is shown in Fig. 6c. The reconstructed results for recorded PSH and engineered PSH are shown in Figs. 6d and 6e respectively. The optimized values of the reconstruction parameters are α = 0.2, β = 1, and n = 9. The DI of object is displayed in Fig. 6f. Comparing the reconstruction results obtained from recorded PSH and engineered PSH, the reconstruction result corresponding to the engineered PSH appears sharper.

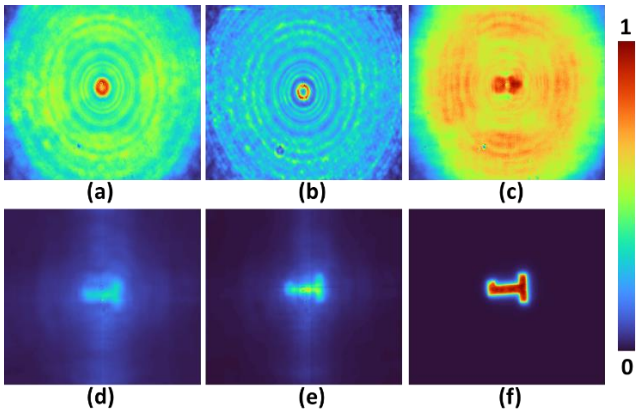

Fig. 6. Simulation results for computational point spread function engineering (CPSFE). (a) PSH obtained for a pinhole with d = 50 µm. (b) Engineered ideal PSH. (c) OH. (d) Reconstruction result using recorded PSH shown in (a). (e) Reconstruction result using ideal PSH shown in (b). (f) Direct imaging.

IV. Conclusion

The most advanced version of FINCH reported as of date is by Tahara, where two camera shots were used for 3D imaging with superior lateral resolution, low axial resolution and low light throughput. In this study, FINCH is realized as CAI and implemented with three algorithms, namely TAP-GSA, LRRA, and CPSFE. The CPSFE technique has been recently demonstrated to improve the SNR of coded aperture holography methods. The CPSFE can also improve advanced holography techniques. In the proposed method, the phase masks generated using TAP-GSA were displayed on the SLM, and the holograms were recorded. TAP-GSA improved the light throughput. The object was reconstructed using the recorded PSH and OH using the LRRA algorithm. The reconstruction with LRRA has a higher SNR than NLR. The experiment was carried out for both single-plane object and two-plane objects. The two-plane experiment revealed the improvement in axial resolution when compared with conventional FINCH. The experimental results prove that FINCH as CAI with the above three algorithms has a higher temporal resolution, higher axial resolution, higher light throughput, same lateral resolution in comparison to conventional FINCH. Implementing FINCH as CAI enabled single-shot capability and improved axial resolution. The TAP-GSA improved the light throughput, LRRA improved the SNR in reconstruction, and CPSFE solved an intrinsic problem in CAI and assisted in retaining the super lateral resolution of FINCH. When all the methods were simultaneously applied, it pushed FINCH beyond the state-of-the-art. We believe that this development will lead to enhanced FINCH-scopes, coded aperture imaging systems and 3D fluorescence microscopes in the future.

Acknowledgment

F. G. A thanks the Computational Imaging and Processing in High Resolution (CIPHR) group for the valuable assistance.

References

[1] J. Rosen, and G. Brooker, “Digital spatially incoherent Fresnel holography,” *Opt. Lett*, vol. 32, no. 8, pp. 912–914, Apr. 2007.

[2] J. Rosen, A. Vijayakumar, M. Kumar, M. R. Rai, R. Kelner, Y. Kashter, A. Bulbul, and S. Mukherjee, "Recent advances in self-interference incoherent digital holography," *Adv. Opt. Photon*, vol. 11, pp. 1-66, Mar. 2019.

[3] J. Rosen, S. Alford, A. Vijayakumar, J. Art, P. Bouchal, Z. Bouchal, M.-U. Erdenebat, L. Huang, A. Ishii, S. Juodkazis, et al, “Roadmap on Recent Progress in FINCH Technology,” *J. Imaging*, vol. 7, no. 10, pp. 197, Sep. 2021.

[4] S. Gopinath, A. Bleahu, T. Kahro, et al. “Enhanced design of multiplexed coded masks for Fresnel incoherent correlation holography,” *Sci Rep*. vol. 13, no. 7390, May 2023.

[5] A. Vijayakumar, M. Han, J. Maksimovic, S. H. Ng, T. Katkus, A. Klein, K. Bambery, M. J. Tobin, J. Vongsvivut, and S. Juodkazis, “Single-shot mid-infrared incoherent holography using Lucy-Richardson-Rosen algorithm,” *Opto-Electron. Sci*, vol.1, no.3, pp. 210006-1 – 210006-8, 2022.